Structure-Aware Halftoning

5 authors, including:

Wai-Man Pang
Caritas Institute of Higher Education
81 PUBLICATIONS **695** CITATIONS

SEE PROFILE

Daniel Cohen-Or
Tel Aviv University
273 PUBLICATIONS **22,567** CITATIONS

SEE PROFILE

Tien-Tsin Wong
The Chinese University of Hong Kong
216 PUBLICATIONS **4,223** CITATIONS

SEE PROFILE

Pheng-Ann Heng
The Chinese University of Hong Kong
549 PUBLICATIONS **11,452** CITATIONS

SEE PROFILE

Some of the authors of this publication are also working on these related projects:

Project   Call for Paper : IMAD 2017 View project

Project   Smart-Toy View project

Structure-Aware Halftoning

Wai-Man Pang[1]   Yingge Qu[1]   Tien-Tsin Wong[1]   Daniel Cohen-Or[2]   Pheng-Ann Heng[1]
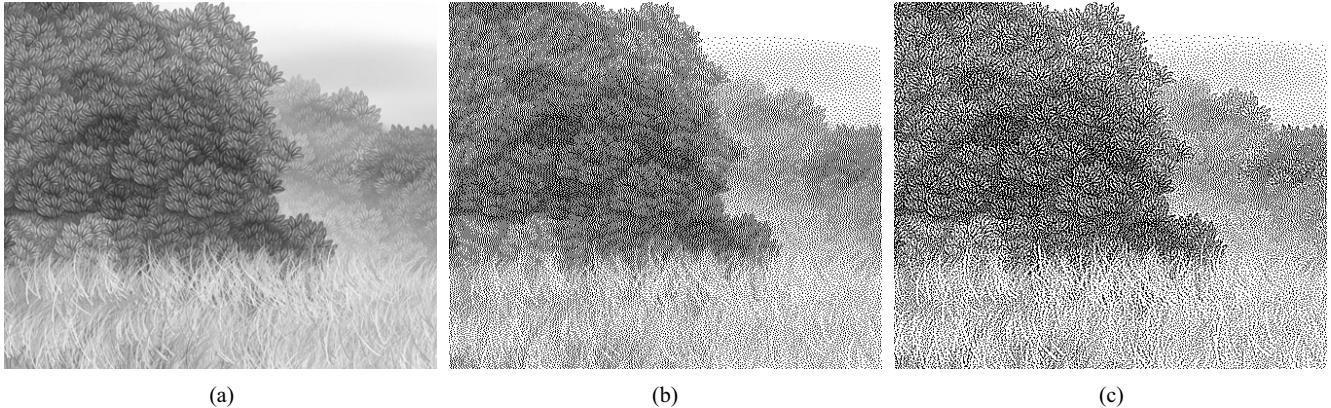[1]The Chinese University of Hong Kong   [2]Tel Aviv University

Figure 1: (a) Original grayscale image. (b) Halftone image by the state-of-art error-diffusion [Ostromoukhov 2001]. (c) Our result. Note that our result faithfully preserves the texture details as well as the local tone. All images have the same resolution of 445×377.

Abstract

This paper presents an optimization-based halftoning technique that preserves the structure and tone similarities between the original and the halftone images. By optimizing an objective function consisting of both the structure and the tone metrics, the generated halftone images preserve visually sensitive texture details as well as the local tone. It possesses the blue-noise property and does not introduce annoying patterns. Unlike the existing edge-enhancement halftoning, the proposed method does not suffer from the deficiencies of edge detector. Our method is tested on various types of images. In multiple experiments and the user study, our method consistently obtains the best scores among all tested methods.

1 Introduction

Halftoning is a heavily used color quantization technique in digital printing and imaging industry. It expresses a grayscale or color image with a reduced number of paints while maintaining a close visual impression to the original image. The key to applying halftoning is spatial integration, in which our human vision system (HVS) perceptually "fuses" the intensity or color of quantized values as viewed from a sufficient distance. Classical halftoning techniques, such as ordered dithering and error diffusion, achieve the tone reproduction based on the principle of spatial integration [Ulichney 1987].

Halftoning algorithms are designed to deal with uniform textureless regions. Graylevel ramps are successfully reproduced by advanced halftoning methods [Ostromoukhov 2001; Mitsa and Parker 1992], without introducing noticeable patterns. However, halftoning techniques typically fail to convey the inherent pattern of textured or structural regions.

A close inspection of the texture regions (e.g. Figure 1(b)) reveals that the halftoning technique destroys the characteristic pattern, and sometimes introduces aliasing artifacts (e.g. Figure 3). Figure 1(c) shows the halftoning result of the technique that we introduce in the paper. As can be clearly seen, this image reproduces the correct tone, and at the same time it is faithful to the original texture look.

Common halftoning techniques suppress the appearance of artifacts at the cost of over-blurring fine texture details. Several methods have been proposed to deal better with texture. These methods [Eschbach and Knox 1991; Hwang et al. 2004; Kwak et al. 2006] rely on edge enhancement techniques. However, edge enhancement provides only a partial solution. As can be observed in Figure 7, it is not sufficient to satisfy the human sensitivity to textures, such as the failure to detect weak edges or improper emphasis of details.

In this paper, we introduce a new approach which optimizes the local spatial distribution of the dots to produce a halftone image that preserves the local tone as well as a resemblance to the original texture, in the expenses of longer execution time. Our method is based on a structure-similarity metrics that respects the human vision sensitive patterns. We formulate the digital halftoning as a minimization of an objective function that accounts for structure-similarity as well as the tone-similarity. We show numerous results of our method applied to a wide variety of images.

2 Related Work

Halftoning has been an active area of research for years [Ulichney 1987; Jarvis et al. 1976]. Classical dithering methods include ordered dithering [Bayer 1973], Floyd-Steinberg error diffusion [Floyd and Steinberg 1974], and Knuth's dot-diffusion [Knuth 1987]. Their primary goal is to retain the local tone of the original image. The main challenge is to reduce the associated noticeable annoying patterns that these methods incur (see Figure 3).

In an effort to alleviate the appearance of these visually unpleasant patterns, researchers applied spectral analysis to measure the quality of the halftone images [Mitchell 1987]. It is accepted that the ideal halftone image has a blue-noise spectrum. Mitsa and Parker [1992] propose to construct a blue noise mask which can produce a blue noise pattern. Geist et al. [1993] introduce a Markovian framework to measure the aesthetics of halftoning, and to optimize the halftone patterns. Ostromoukhov [2001] extends the standard error-diffusion method with variable diffusion factors for different intensity levels and gracefully creates a blue noise pattern.

Li and Allebach [2002] design a tone-dependent error-diffusion method with the optimal error weighting and thresholding obtained from the references. These references are the halftone result from direct binary search, an iterative optimization method with neighbor pixel-swapping. Baqai and Allebach [2003] incorporate printer models with the direct binary search method to enhance the detail rendition and tonal gradation. Zhou and Fang [2003] demonstrate a variable threshold modulation method for removing artifact in halftoning, especially at midtones. Kopf et al. [2006] propose a recursive tiling approach for fast generation of blue noise. We regard the halftoning technique of Ostromoukhov [2001] to be the current state-of-the-art halftoning method. In our work, we compare our results with this technique (e.g., Figure 1).

Although halftoning with blue noise properties can suppress many of the annoying patterns, it may at the same time over-blur the fine texture details in the original images. To alleviate this problem and to better deal with textures, recent methods preserve the structural details via edge enhancement. Eschbach and Knox [1991] improve the basic error diffusion mechanism by modulating the thresholding process with the edge response. However, since the modulation is applied uniformly over the whole image, low-frequency regions are affected as well. Figures 4, 7, and 12-15 show some of the results using this edge enhancement halftoning method. Hwang et al. [2004] improve the above method by considering spatial information as well. However, their method may sometimes blur the edges. To reduce this defect, Kwak et al. [2006] improve the method by considering both the local luminance average and variation. Li [2006] proposes to explicitly extract a binary edge map to guide the error diffusion process. Although these methods generate halftoning images with stronger edges, their performance directly depends on the reliability of the edge detection operator. Moreover, preserving edges is not necessarily equivalent to preserving human vision sensitive textures in the original images as demonstrated in Figure 7. The method we introduce in the paper directly targets texture and preserves it by optimizing the halftoning.

Another class of halftoning techniques aims at the artistic applications [Ostromoukhov and Hersch 1995; Pnueli and Bruckstein 1996; Verevka and Buchanan 1999]. Their goal is to produce tone-preserved screening with specific artistic patterns provided by the user. An interesting technique in non-photorealistic rendering is stippling [Deussen et al. 2000; Secord 2002]. This method can be regarded as a special type of artistic halftoning with an emphasis on the aesthetic distribution of the dots or other small icons.

3 Structure-aware Halftoning

Images are not aggregates of smooth pieces, they typically contain textured regions. Textures consist of particular high-frequency patterns which our visual system is sensitive to. To preserve the characteristic look of these textured regions in a halftone image, we present here a structure-aware halftoning technique. The goal is to optimize the placement of the black dots in a bi-tonal halftone image to better express the textures in the original grayscale image. The challenge is to distribute the black dots so that locally they are perceived to be similar to graylevel textures, and at the same time their local tone needs to be preserved. Our approach is to directly optimize an objective function that respects both the tone and the texture. That is, the objective function consists of two terms: a tone term and a structure term. While the first is quite simple to define, the latter requires special care as there is no definite way to measure distances among textures.

The basic concept of tone-aware halftoning is based on the spatial integration response of the human vision systems (HVS) to halftone images [Ulichney 1987]. It is well-known that the spatial integration of HVS is very much like the effect of Gaussian

filter. Similarly, a structure-aware halftoning requires a measure that respects the HVS so that the textures of the halftoning image are perceived as the original. The structure measure that we use in our work is based on the structural similarity measure (SSIM) introduced by Wang et. al. [2004]. While most image-based distance measures use pointwise signal differences (e.g., Mean Square Error or MSE), the SSIM considers image degradations as perceived changes in structural information variation. Figure 2 depicts the power of SSIM. The three images in (b-d) have the same MSE. Clearly the MSE is not sensitive to the human visual system, while the SSIM is intuitive and yields a consistent perceived visual error.
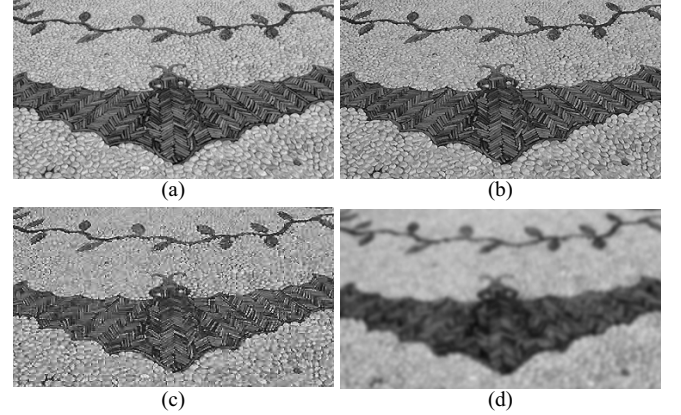

(a)   (b)

(c)   (d)

Figure 2: MSSIM comparison of image "bat" contaminated with different types of distortions, all with the same MSE. (a) Original image; (b) Contrast-stretched image, MSSIM = 0.9640; (c) JPEG compressed image (with low quality), MSSIM = 0.6834; (e) Blurred image, MSSIM = 0.2827.

Optimization   Given a grayscale image I, the corresponding halftone image I_h is obtained by minimizing the following objective function:

$$\text{Objective}(I, I_h) = w_g G(I, I_h) + w_t (1 - \text{MSSIM}(I, I_h)), \quad (1)$$

where $G(I, I_h)$ measures the tone similarity between the original and the halftone images; and $\text{MSSIM}(I, I_h)$ measures the structure similarity. These two terms are described in detail in the following subsections. The w_g and w_t are the weighting factors, such that $w_g + w_t = 1$. In all our experiments, we set $w_t = w_g = 0.5$.

Our optimization can start with any bi-tonal image with global grayness (ratio of black to white pixels) equivalent to that of the original grayscale image. Such initialization can be done by randomly distributing black/white pixels such that the overall grayness is maintained. For faster convergence, we may also start with the halftoning result of an existing method, such as the state-of-the-art error diffusion by Ostromoukhov [2001].

We minimize the objective function using a simulated annealing strategy. In each iteration, we randomly pick a pair of black and white pixels from the image and swap them. Then we test whether the swapping decreases the objective function. If not, the swapping is undone. Since no extra black or white pixel is introduced, the overall grayness should be maintained.

Structure Similarity   We employ the structural similarity index measure (SSIM) [Wang et al. 2004] to quantify the structure difference between the halftone result and the original grayscale image. For each corresponding pair of pixels from the two given images, the SSIM measures the local structure similarity in their local neighborhoods (x and y). In our case, we use a neighborhood window of size 11×11. The basic idea of SSIM is to separate the task of similarity measurement into three comparisons: luminance, contrast and structure.

Suppose x and y are two nonnegative aligned image signals, each with N elements. First, the luminance of each signal is compared. This is estimated using the weighted mean intensity $\mu_x = \sum_{i=1}^{N} w_i x_i$. Usually a normalized Gaussian weighting is used. The luminance comparison function $l(x,y)$ is then a function of μ_x and μ_y as in Equation 2.

$$l(x,y) = \frac{2\mu_x\mu_y + k_1}{\mu_x^2 + \mu_y^2 + k_1}, \tag{2}$$

where k_1 is a small constant to avoid singularity. The formulation is qualitatively consistent with Webers law, which models light adaptation in the HVS, as HVS is more sensitive to relative luminance change rather than the absolute one.

The contrast comparison $c(x,y)$ has the similar formulation, but it makes use of the standard deviation σ_x and σ_y as an estimate of the signal contrast.

$$c(x,y) = \frac{2\sigma_x\sigma_y + k_2}{\sigma_x^2 + \sigma_y^2 + k_2}, \quad \sigma_x = \left(\sum_{i=1}^{N} w_i(x_i - \mu_x)^2\right)^{\frac{1}{2}} \tag{3}$$

where k_2 is a small constant avoiding singularity.

The correlation between the images is used as a simple and effective measure to quantify the structural similarity. Thus, the structure comparison function is defined as follows:

$$s(x,y) = \frac{\sigma_{xy} + k_3}{\sigma_x\sigma_y + k_3}, \quad \sigma_{xy} = \sum_{i=1}^{N} w_i(x_i - \mu_x)(y_i - \mu_y). \tag{4}$$

where σ_{xy} defines the inner product, and k_3 is a small constant avoiding singularity.

The three components are combined by simple multiplication to yield an overall similarity measure. Expanding it using Equations 2, 3, 4 and $k_3 = k_2/2$ yields the following equation:

$$\begin{aligned} \text{SSIM}(x,y) &= l(x,y) \cdot c(x,y) \cdot s(x,y) \\ &= \frac{(2\mu_x\mu_y + k_1)(2\sigma_{xy} + k_2)}{(\mu_x^2 + \mu_y^2 + k_1)(\sigma_x^2 + \sigma_y^2 + k_2)} \end{aligned} \tag{5}$$

Note that the three components are relatively independent. For example, the change of luminance or contrast does not affect the structure of the image. Finally, a mean SSIM (MSSIM) that evaluates the overall image quality is obtained by taking the average over all pixels. The valid range of MSSIM is $[0,1]$, with higher values indicating higher similarity.

Tone Similarity The above MSSIM cannot directly account for the tone similarity, as the luminance component l is modulated by the contrast c and structure s terms. Therefore, a simple tone similarity term G is introduced into the objective function. Term $G(I,I_h) = \frac{1}{M}\sum^M(g(I) - g(I_h))^2$ measures the tone preservation, with valid range in $[0,1]$. It measures the MSE between the Gaussian-blurred grayscale input $g(I)$ and the Gaussian-blurred halftone image $g(I_h)$. In our implementation, a Gaussian kernel of size 11×11 is employed.

Algorithm Listing 1 presents the pseudo-code for our algorithm. The function `TonePreserveInit` initializes the halftone image by randomly distributing black and white pixels. The only criterion is to maintain the overall grayness, so that it is equivalent to that of the original grayscale image. This ensures the overall image grayness is preserved.

In each iteration, an arbitrary pair of black and white pixels is swapped (`RandomSwap`). The swapping is being accepted or rejected according to a simulated annealing strategy. A certain number of iterations (K) is performed at a certain *temperature* before the next annealing. Specifically, we set K equals number of pixels. Function `UndoSwap` undoes the swapping whenever the swap does not improve. In our implementation, we use 0.8 and 0.01 for the *AnnealFactor* and *limit* respectively.

Listing 1 Pseudo-code of optimization

```
Initialize I_h by TonePreserveInit(I)
E_old =Objective(I , I_h)
temperature = 0.2
Loop ( temperature > limit )
    Loop (K times)
        I_h = RandomSwap();
        E_new =Objective(I,I_h)
        ΔE = E_new − E_old
        // Accept or Reject according to annealing strategy
        If (random()< e^{min(0,−ΔE/temperature)} )
            E_old = E_new;
        else
            UndoSwap();
        temperature = AnnealFactor × temperature;
```

---

4 Results and Analysis

To verify the performance of our method, we tested it on examples with different natures, including photographs, paintings, and illustrations. Besides the subjective visual comparison, we also carry out more objective evaluations including the tone consistency, structural preservation, blue-noise analysis, and a user study. All tested images in this paper are initialized with the halftone results by Ostromoukhov method, except the ones in Figures 8 and 9.

Visual Comparison Figures 3, 4 and 12-15 visually compare our results to that of the error-diffusion based method by Ostromoukhov [2001] and an advanced edge-enhancement based method [Eschbach and Knox 1991]. We generally leave out the results of ordered dithering for the sake of space, since they are clearly outperformed by the Ostromoukhov's method. The edge enhancement halftone method that we used for comparison is implemented according to [Ostromoukhov 2001]. It is a modified Ostromoukhov method with the threshold modulation introduced in [Eschbach and Knox 1991] in order to control the inherent edge enhancement.

In general, and in particular for all tested images, our method preserves more structural details than that of Ostromoukhov method and ordered dither. The edge enhancement method, unlike our method, may over-emphasize the edges (Figure 14) and degrade the resemblance to the original grayscale image. Since the edges are detected with a threshold, the edge enhancement method may fail to preserve the weak edges and blurry regions (Figure 7).

Figure 3 shows the gray ramp example and the corresponding halftone images produced by different methods. In this textureless example, since there are no edges, we compare to the ordered dither instead of the edge enhancement method (which otherwise generates the same result as Ostromoukhov method). The performance of our method is comparable to the Ostromoukhov method.

Tone Consistency We first evaluate the preservation of image intensity. Note that both the tone consistency and structure preservation evaluations are incorporated inside our objective function. Our optimization strikes a balance between these two metrics. In this experiment, we *separately* measure the tone consistency among all tested methods. We measure the difference between the Gaussian-filtered grayscale and the Gaussian-filtered halftone images. The PSNRs of halftone images produced by all four methods are tabulated and plotted in Figure 5. Some of the eight tested grayscale images can be referred in Figures 4, 12-15. From the statistics, our results consistently obtain high PSNRs (highest PSNR in 7 out of 8 trials).
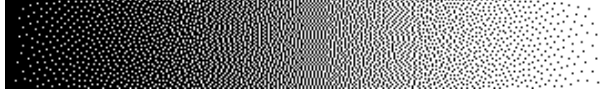
Ramp(0-255)

Ordered dither
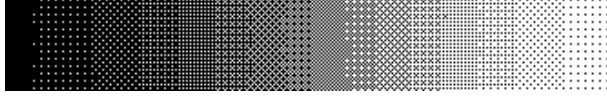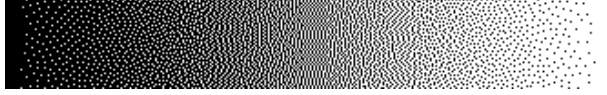
Ostromoukhov method

Our method

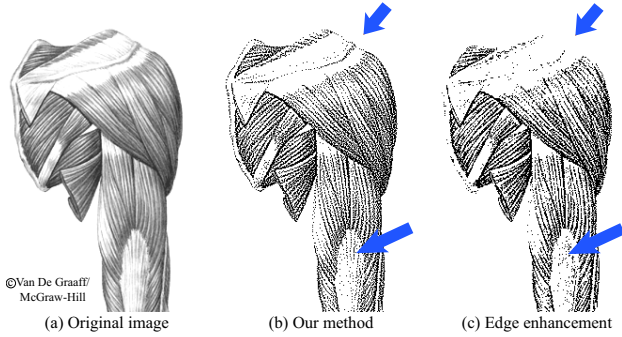Figure 3: Gray ramps. All images have the same resolution of 400×74.

©Van De Graaff/
McGraw-Hill

(a) Original image   (b) Our method   (c) Edge enhancement

Figure 4: Image "arm". (a) Original, (b) our method, and (c) edge enhancement. All images have the same resolution of 200×307.

Structure Preservation To measure the structure preservation, we employ the MSSIM measurement. Here the MSSIM is measured independently, learning whether the optimization succeed in preserving the structure while preserving the tone at the same time. Figure 6 tabulates and plots the MSSIM values for the same set of test images. As can be seen, the performance of our method is generally better than that of the edge-enhancement method.

Although the performance of edge enhancement halftoning is close to ours, it suffers in areas with blurriness and weak edges. Figure 7(a) shows the annoying patterns introduced at the blurry region while Figure 7(b) shows its failure to track the weak edges. In contrast, our method faithfully preserves the weak edges as well as the blurry region.

Blue-Noise Analysis Blue-noise property is commonly used in measuring the quality of halftoning methods [Ulichney 1987]. To measure the blue-noise property, we compute the Fourier spectrum and radially averaged power spectra of the halftoning results. The radially averaged power spectra is usually used to visualize the blue noise property in 1D. This 1D spectra is derived from the estimated 2D power spectrum $P(f)$, which is computed using the Fourier amplitude spectrum and the Bartlett's method [Bartlett 1955] of averaging periodograms. The power spectrum is first partitioned radially into many annuli. Then, the radially averaged power spectra is defined as follow

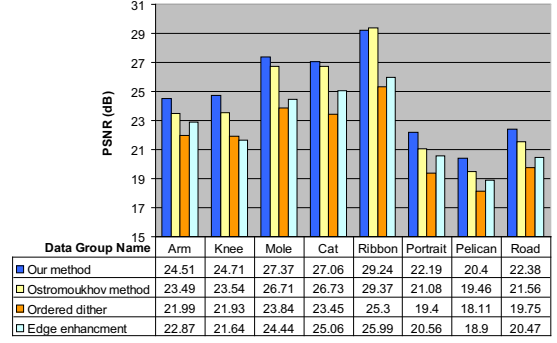$$P_r(f_r) = \frac{1}{N_r(f_r)} \sum_{i=1}^{N_r(f_r)} P(f). \quad (6)$$
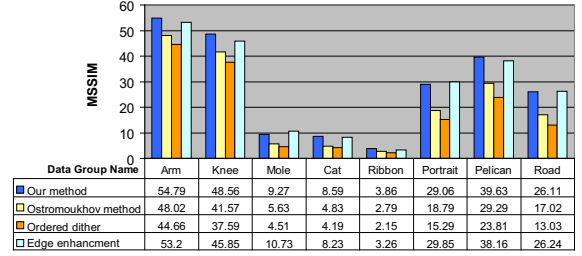

Figure 5: PSNR comparison.

Data Group Name	Arm	Knee	Mole	Cat	Ribbon	Portrait	Pelican	Road
Our method	24.51	24.71	27.37	27.06	29.24	22.19	20.4	22.38
Ostromoukhov method	23.49	23.54	26.71	26.73	29.37	21.08	19.46	21.56
Ordered dither	21.99	21.93	23.84	23.45	25.3	19.4	18.11	19.75
Edge enhancment	22.87	21.64	24.44	25.06	25.99	20.56	18.9	20.47

Figure 6: MSSIM comparison.

Data Group Name	Arm	Knee	Mole	Cat	Ribbon	Portrait	Pelican	Road
Our method	54.79	48.56	9.27	8.59	3.86	29.06	39.63	26.11
Ostromoukhov method	48.02	41.57	5.63	4.83	2.79	18.79	29.29	17.02
Ordered dither	44.66	37.59	4.51	4.19	2.15	15.29	23.81	13.03
Edge enhancment	53.2	45.85	10.73	8.23	3.26	29.85	38.16	26.24

The sample mean is computed for each annulus with a central radius f_r (also refer to as radial frequency). Here, $N_r(f_r)$ is the frequency samples within the annulus of f_r.

As Ostromoukhov method is well-known in maintaining the blue-noise property, it is compared to our method in this blue-noise analysis (Figure 8). A constant-grayness image is processed to produce the halftone images in this test. In order to give a fair comparison without the influence from Ostromoukhov method, our halftone image is initialized as a random noise (Figure 8). Both results show the similar blue noise profile, i.e. low energy characteristics at low frequencies. The underlying reason of our objective function being able to maintain the blue-noise property is due to its structure term. When the dots are not evenly distributed (e.g. dots clump or align to form line/curves) in the halftone result, it exhibits significant difference, in terms of SSIM value, comparing to the original smooth grayscale image. Hence, to maintain a close SSIM value to the original smooth grayscale, the dots push away from each other (like Poisson disk) and result in maintaining the blue-noise property. This is evidenced by the sequence in Figure 9 that shows how the white-noise initial converges to a blue-noise result.

User Study We further conducted a user study to learn whether the structure-aware halftoning preserves better structural contents than other methods from the user point of view. Eight different subjects were asked to rate a 9-point scale ([1-9] with 9 as more similar) for the texture and tone similarities of original grayscale and the halftone images. Again, ordered dither, Ostromoukhov method, edge enhancement halftoning, and our method were compared. We presented each halftone result to the subjects with the original grayscale image beside, and they were asked to rate without telling which technique was used. Twelve sets of test images were used, so there were altogether 96 data samples for analysis. Table 1 shows the statistics from the collected data.

From Table 1, the mean scores for structure-aware halftoning, Ostromoukhov method, edge enhancement halftoning, and ordered dither are 7.22, 6.59, 6.02, and 4.79, respectively. ANalysis Of VAriance (ANOVA) is used to test if the difference of the means
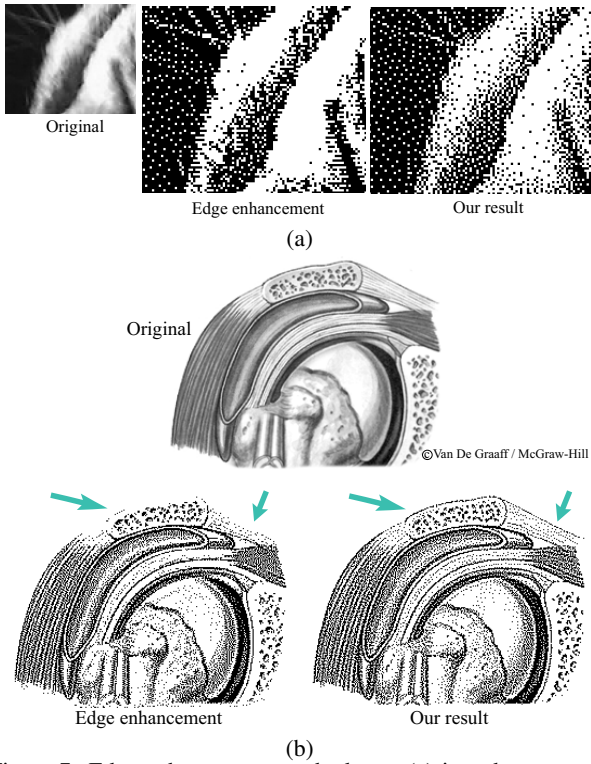
Figure 7: Edge enhancement method may (a) introduce annoying pattern at blurry regions and (b) fail to track the weak edges. Resolution of all images in (a) is 294×245, and (b) is 269×203.

are statistically significant, under the assumption that the sampled populations are Gaussian distributed. The F value is the test statistic used to decide whether the sample means are within sampling variability of each other, and it is computed as follow,

$$F(k-1, n-k) = \frac{\sum n_i (\overline{x_i} - \overline{x})^2 / (k-1)}{\sum (n_i - 1) s_i^2 / (n-k)} \quad (7)$$

Here n is the total number of data samples in comparison. k is the number of groups in comparison, we have four in total for the tested halftone methods. $\overline{x_i}$ is the mean value for group i (e.g. our method has the mean 7.22), $\overline{x}$ is the mean for all data samples. s_i is the standard deviation for group i. ANOVA result among the four groups is $F(3, 380) = 69.088$, $p < 0.001$, this reveals that there is a significant difference in the four group means. When comparing our method to error diffusion ($F(1, 190) = 16.681$, $p < 0.001$), edge enhancement ($F(1, 190) = 69.478$, $p < 0.001$) or ordered dither ($F(1, 190) = 139.094$, $p < 0.001$), our ANOVA result is also significant. From the 95% confidence interval, it can be shown that the result of structure-aware halftoning is clearly more perceptually similar to the original than that of other methods.

Degree of Structure Preservation Halftoning for artistic purpose usually favors texture details, in additional to the tone. So in this experiment, we try to observe the degree of structure detail preservation, by adjusting the weighting factors w_g and w_t. Recall that $w_g + w_t = 1$. Figure 10 shows halftone results of using different weighting values. The texture is not apparent when w_t is 0.1. As we further increase w_t, more texture details are preserved in the generated halftone images. It can be observed that the degree of texture preservation seems to be saturated after $w_t > 0.5$. All the images generated in this paper use the same value $w_t = 0.5$.
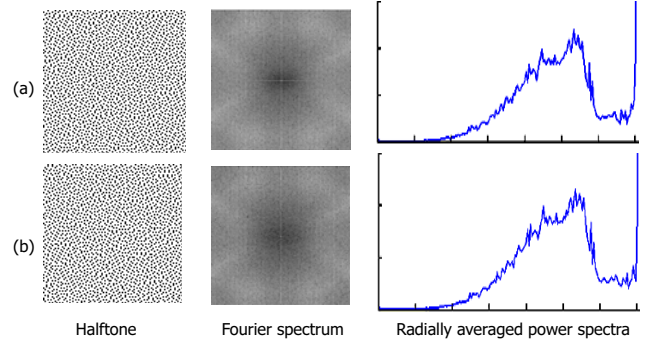
Figure 8: A spectral analysis of halftoning a constant-grayness image (grayness=0.75). (a) and (b) show the analysis of Ostromoukhov method and our method respectively. From left to right, the halftone image, 2D Fourier amplitude spectrum, and the radially averaged power spectra are shown.
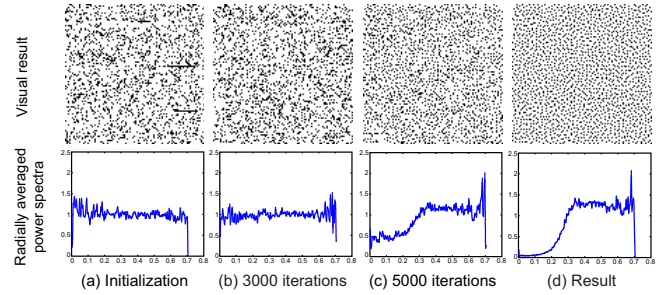

Figure 9: From white noise to blue noise. The input is a textureless image with constant grayness of 0.82. From left to right, the halftone result converges from the white-noise initial to the blue-noise result. The corresponding radially averaged power spectra are shown underneath.

Color Halftone Our method can be naturally extended to color halftoning. The general idea is the same. By optimizing the distribution of four primary printed color dots, cyan, magenta, yellow, and black (CMYK), we make a balance between the color tone and the structure similarity. Note that, we perform the adjustment in CMYK space, but we evaluate the objective function in RGB space. The rationale is that our retina are equipped with three types of color receptors responsible for long (R), medium (G), and short (B) wavelengths, and hence our HVS is better explained in RGB space.

We generate the initialization of CMYK according to [Shaked et al. 1996], then perform our optimization on each subtractive color. The objective function is rewritten as:

$$\text{Objective}(I, I_h) = w_g G_{RGB}(I, I_h) + w_t (1 - \text{MSSIM}_{RGB}(I, I_h)), \quad (8)$$

where I and I_h are both in RGB space; G_{RGB} is the color version of G. It is simply the summation of G running over R, G, and B channels separately. MSSIM_{RGB} is defined similarly. Figure 11

Method	Mean	Standard Deviation	95% Confidence Interval	
			Lower Bound	Upper Bound
Our method	7.22	1.08	6.99	7.43
Ostromoukhov	6.59	1.03	6.38	6.80
Edge enhancement	6.02	0.89	5.83	6.20
Ordered dither	4.79	1.69	4.44	5.13

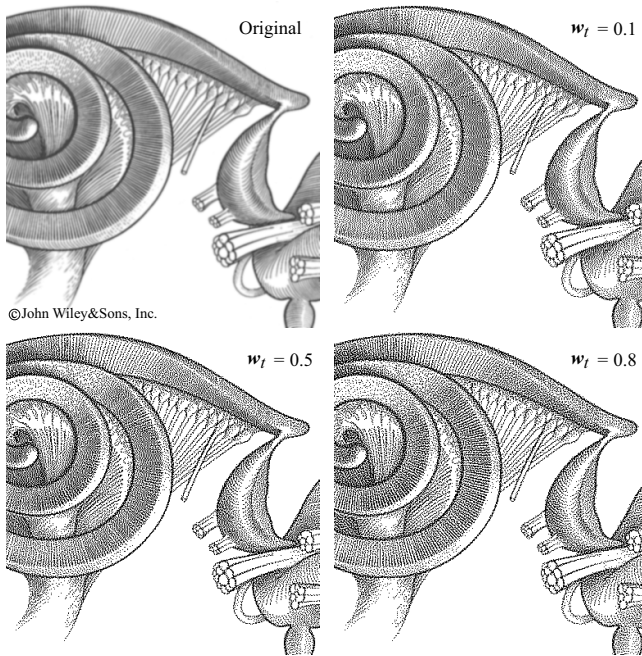Table 1: User study statistics. The mean value shows the similarity to the original image.

Figure 10: "Snail shaped organ". Halftoning with different structure weights.

(a) Original image   (b) Our method   (c) Color error diffusion

Figure 11: Structure-aware color halftoning. The resolution of all halftone images is 200×307.

shows our result in (b), and the color error diffusion in (c) [Shaked et al. 1996].

Limitation   Although our method is better than existing methods in preserving texture and tone, our technique does not accommodate the internal issues of printers which may not use simple grids. Moreover, in our current implementation, the weighting factor is homogenously applied to the whole image. In some cases, it may be desirable to adjust the degree of structure preservation in a spatial varying manner. Our method is more expensive on timing due to the iterative nature. The time required to generate a 256×256 image is 27 seconds, and for a 512×512 image is 2 minutes, with our current software implementation on a PC equipped with Intel P4 3.2GHz CPU and 2GB memory.

5   Conclusion

In this paper, we presented an optimization-based method for maintaining structure as well as the tone similarity. Compared to the standard ordered dither and the state-of-the-art error diffusion, our method preserves better texture content that is sensitive to HVS, and at the same time, possesses the blue-noise property. Compared to previous edge-enhancement based halftoning, our method does not suffer from the deficiency of edge detector. With the support of experiments and user study, our method outperforms alternative methods and presents visually appealing results. One possible future direction is to adaptively adjust the degree of structure preservation in a spatial-varying manner. A fully automatic approach may require further study in visual perception, while an interactive approach could be useful for users to control the appearance of texture details at different regions of the image.

References

BAQAI, F., AND ALLEBACH, J. 2003. Halftoning via direct binary search using analytical and stochastic printer models. *IEEE Transactions on Image Processing 12* (January), 1–15.

BARTLETT, M. S. 1955. *Introduction to Stochastic Processes with Special Reference to Methods and Applications*. Cambridge University Press, New York.

BAYER, B. 1973. An optimum method for two-level rendition of continuous-tone pictures. In *IEEE International Conference on Communications*, IEEE, (26–11)–(26–15).

DEUSSEN, O., HILLER, S., VAN OVERVELD, C., AND STROTHOTTE, T. 2000. Floating points: A method for computing stipple drawings. *Computer Graphics Forum 19*, 3, 40–51.

ESCHBACH, R., AND KNOX, K. T. 1991. Error-diffusion algorithm with edge enhancement. *J. Opt. Soc. Am. A 8*, 12, 1844.

FLOYD, R. W., AND STEINBERG, L. 1974. An adaptive algorithm for spatial grey scale. In *SID International Symposium Digest of Technical Papers*, Society for Information Display, 36–37.

GEIST, R., REYNOLDS, R., AND SUGGS, D. 1993. A markovian framework for digital halftoning. *ACM Trans. Graph. 12*, 2, 136–159.

HWANG, B.-W., KANG, T.-H., AND LEE, T.-S. 2004. Improved edge enhanced error diffusion based on first-order gradient shaping filter. In *IEA/AIE'2004: Proceedings of the 17th international conference on Innovations in applied artificial intelligence*, Springer Springer Verlag Inc, 473–482.

JARVIS, J. F., JUDICE, C. N., AND NINKE, W. H. 1976. A survey of techniques for the display of continuous tone pictures on bilevel displays. *Comput Graphics Image Process 5*, 1, 13–40.

KNUTH, D. E. 1987. Digital halftones by dot-diffusion. *ACM Transactions on Graphics 6*, 4, 245–273.

KOPF, J., COHEN-OR, D., DEUSSEN, O., AND LISCHINSKI, D. 2006. Recursive wang tiles for real-time blue noise. In *SIGGRAPH '06: ACM SIGGRAPH 2006 Papers*, ACM, New York, NY, USA, 509–518.
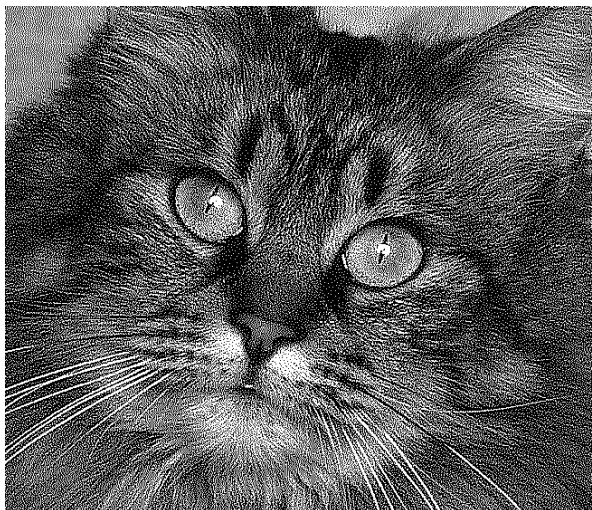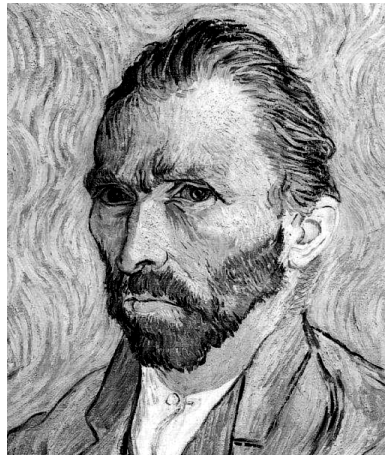
(a) Original Image
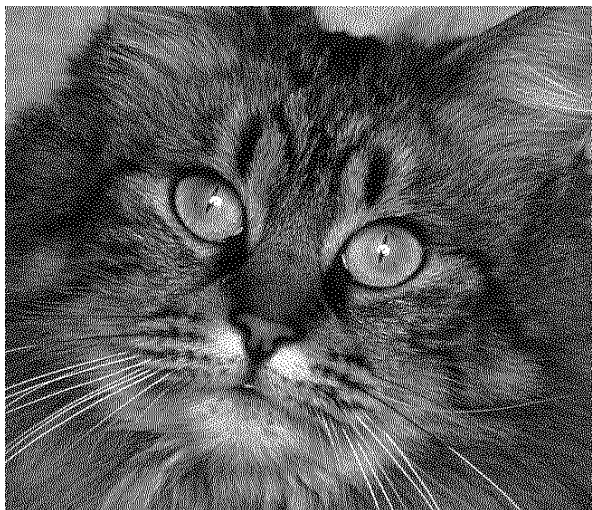
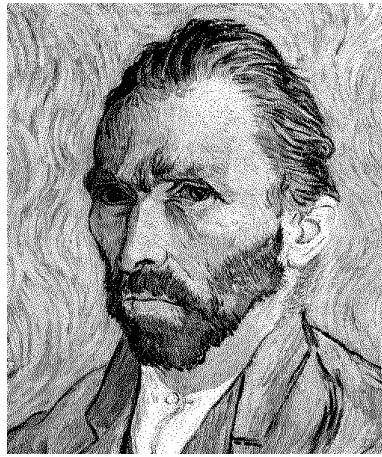(b) Ostromoukhov method
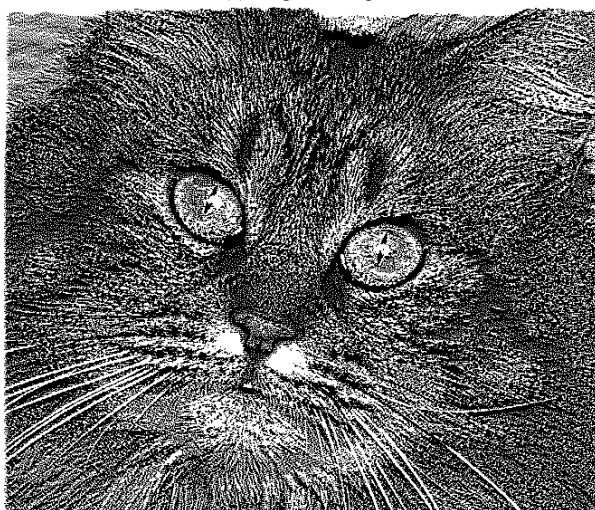
(c) Edge enhancement

(d) Our method

Figure 12: Furry "cat". All images have the same resolution of 660×560.

KWAK, N.-J., RYU, S.-P., AND AHN, J.-H. 2006. Edge-enhanced error diffusion halftoning using human visual properties. In *ICHIT '06: Proceedings of the 2006 International Conference on Hybrid Information Technology*, IEEE Computer Society, Washington, DC, USA, 499–504.

LI, R., AND ALLEBACH, J. 2002. Tone dependent error diffusion. In *Proceedings SPIE Cot Electronic Imaging, (San Jose, CA)*, 293–301.

LI, X. 2006. Edge-directed error diffusion halftoning. *IEEE Signal Processing Letters 13*, 11 (November), 688–690.

MITCHELL, D. P. 1987. Generating antialiased images at low sampling densities. In *Proceedings of SIGGRAPH'87*, vol. 21.

MITSA, T., AND PARKER, K. J. 1992. Digital halftoning technique using a blue-noise mask. *J. Opt. Soc. Am. A 9*, 11, 1920.

OSTROMOUKHOV, V., AND HERSCH, R. D. 1995. Artistic screening. In *SIGGRAPH '95: Proceedings of the 22nd annual conference on Computer graphics and interactive techniques*, ACM, New York, NY, USA, 219–228.

OSTROMOUKHOV, V. 2001. A simple and efficient error-diffusion algorithm. In *SIGGRAPH '01: Proceedings of the 28th annual conference on Computer graphics and interactive techniques*, ACM, New York, NY, USA, 567–572.

PNUELI, Y., AND BRUCKSTEIN, A. 1996. Gridless half-toning: A reincarnation of the old method. 38–64.

SECORD, A. 2002. Weighted voronoi stippling. In *NPAR '02: Proceedings of the 2nd international symposium on Non-photorealistic animation and rendering*, ACM, New York, NY, USA, 37–43.

SHAKED, D., ARAD, N., FITZHUGH, A., AND SOBEL, I. 1996. Color diffusion: Error-diffusion for color halftones. *HP Labs Tech. Report HPL-96-128R1*.

ULICHNEY, R. A. 1987. *Digital Halftoning*. MIT Press, Cambridge, MA.

VEREVKA, O., AND BUCHANAN, J. W. 1999. Halftoning with image-based dither screens. In *Proceedings of the 1999 conference on Graphics interface '99*, Morgan Kaufmann Publishers Inc., San Francisco, CA, USA, 167–174.

WANG, Z., BOVIK, A., SHEIKH, H., AND SIMONCELLI, E., 2004. Image quality assessment: From error visibility to structural similarity.

ZHOU, B., AND FANG, X. 2003. Improving mid-tone quality of variable-coefficient error diffusion using threshold modulation. In *SIGGRAPH '03: ACM SIGGRAPH 2003 Papers*, ACM, New York, NY, USA, 437–444.
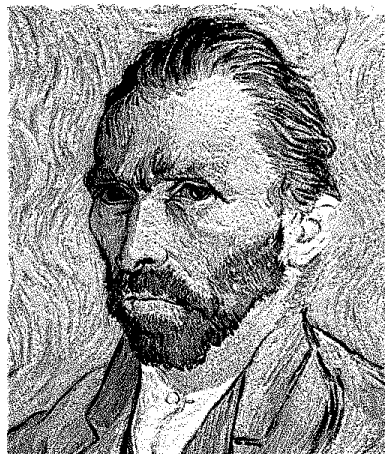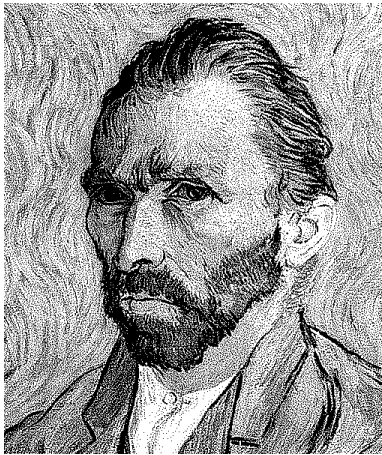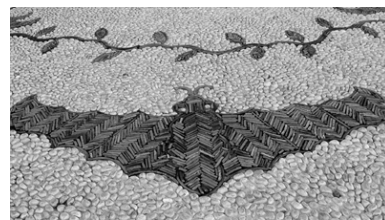
Figure 13: Vincent van Gogh's "Portrait". The resolution of all images is 508x603.
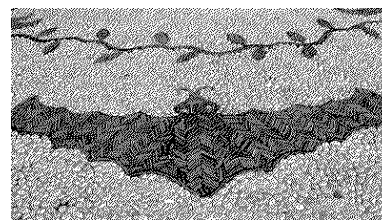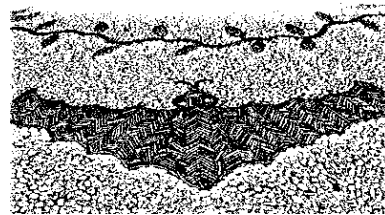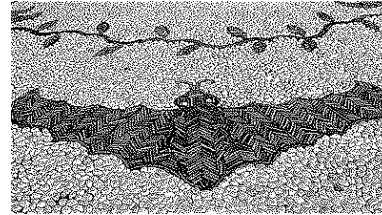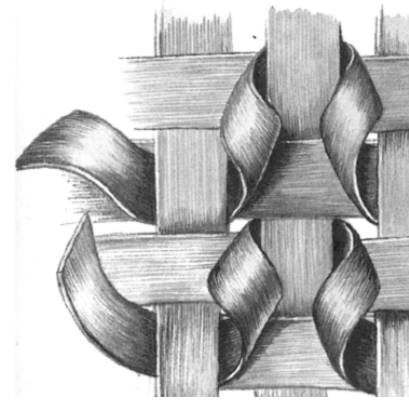

Figure 14: A natural photo of stone art "bat". The resolution of all images is 400x223.
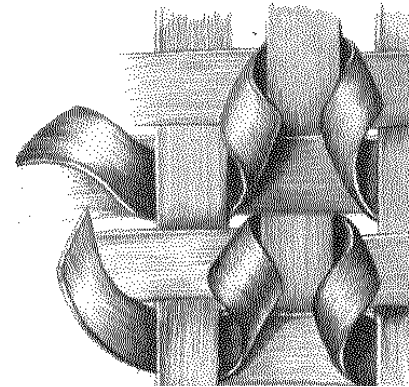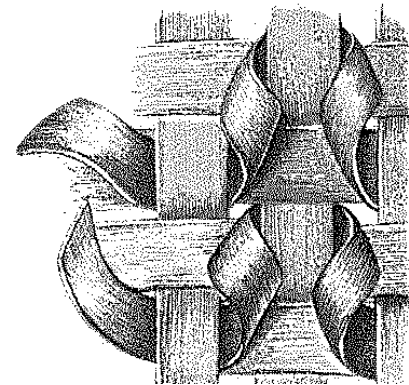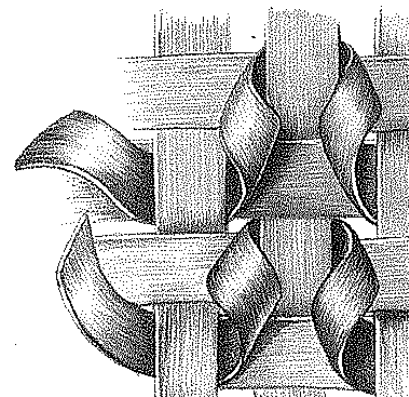
Figure 15: Illustration "ribbon".
The resolution of all images is 367x373.